

This is the accepted manuscript made available via CHORUS. The article has been published as:

# Effect of correlations on electronic structure and transport across (001) Fe/MgO/Fe junctions

Sergey V. Faleev, Oleg N. Mryasov, and Mark van Schilfgaarde

Phys. Rev. B **85**, 174433 — Published 25 May 2012

DOI: [10.1103/PhysRevB.85.174433](https://doi.org/10.1103/PhysRevB.85.174433)

# Effect of electron correlations on (001) Fe/MgO interfaces.

Sergey V. Faleev,<sup>1,\*</sup> Oleg N. Mryasov,<sup>1,†</sup> and Mark van Schilfgaarde<sup>2</sup>

<sup>1</sup>*Physics and Astronomy, University of Alabama, Tuscaloosa, AL, 35487, USA*

<sup>2</sup>*Arizona State University, Tempe, Arizona, 85287, USA*

We developed a parametrization of transmission probability that reliably captures essential elements of the tunneling process in magnetic tunnel junctions. The electronic structure of Fe/MgO system is calculated within the quasiparticle self-consistent *GW* approximation and used to evaluate transmission probability across (001) Fe/MgO interface. The transmission has a peak at +0.12 V, in excellent agreement with recent differential conductance measurements for electrodes with antiparallel spin. These findings confirm that the observed current-voltage characteristics are intrinsic to well defined (001) Fe/MgO interfaces, in contrast to previous predictions based on the local spin-density approximation, and also that many-body effects are important to realistically describe electron transport across well defined metal-insulator interfaces.

PACS numbers: 71.15.-m, 73.20.-r

Energy dissipation in switching a logic unit (transistor) is perhaps the most important bottleneck to continued realization of Moore's law scaling in the density of integrated circuits<sup>1,2</sup>. New materials with special, well defined interfaces<sup>3</sup> and functional properties<sup>4</sup> offer promising routes to circumvent losses. Most new schemes exploit tunneling phenomena across metal-insulators or semiconductor interfaces, so they will play an increasingly important role as we explore fundamental limits of density (miniaturization) in integrated circuits<sup>2</sup>.

In thin FM/insulator/FM heterostructures, where an FM is a ferromagnet, spin polarized electron tunneling is observed. In such "magnetic tunnel junctions" (MTJs) the tunneling resistance changes when alignment of the two FM electrodes are switched from an anti-parallel configuration (APC) to a parallel configuration (PC). This property is encapsulated in the tunneling magnetoresistance (TMR),  $T^{MR} = (G_P - G_A)/G_A$ .  $G_P$  and  $G_A$  are conductivities in the PC and APC<sup>7,8</sup>. These heterostructures are of particular technological interest because of the recent discovery of very large TMR in highly crystalline (001) Fe/MgO/Fe MTJs<sup>9,10</sup>. Equally important to the large TMR is the record low critical current needed to manipulate (switch) magnetization without external magnetic field, relative ease of fabrication and reproducibility<sup>11</sup>. At a fundamental level, the (001) Fe/MgO/Fe system presents an excellent opportunity to investigate the role of the interface and test our ability to predict critical properties controlling transport in a heterostructure with well defined interfaces<sup>9</sup>.

The local spin density approximation (LSDA) has been used to predict TMR in Fe/MgO/Fe system<sup>13-17</sup>. Reports are largely in agreement with each other but at variance with differential conductance measurements for thin MTJs<sup>12,18</sup>. The LSDA predicts a narrow band of interface resonance states (IRS) of minority electrons (Fig. 1) which overlaps the Fermi level  $E_F$ . This prediction has two consequences: first, a sharp reduction in TMR at voltages on the order of  $\sim 0.02$  V, due to sharp (resonant) reduction in minority spin contribution to differential conductance in PC<sup>15,18</sup>. It is called the 'zero-

bias anomaly'. Secondly, it predicts a rise in TMR at larger voltage,  $\sim 0.1$  V, due to reduction in differential conductance in APC<sup>15</sup>. Neither effect has been observed experimentally; instead differential conductance in APC increases monotonically, with  $d^2I/dV^2$  reaching a peak near 0.12 V<sup>12</sup> or 0.15 V<sup>18</sup>. Zermatten et al. attributed this effect to interface states, observed at the (001) Fe free surface by STM measurements.

The absence of 'zero-bias anomaly' in PC is usually explained as a slight asymmetry of the electrodes from e.g., disorder, which breaks matching of the resonant states. Thus for any applied bias the minority-spin contribution to current in PC is much smaller than the majority-spin contribution for MgO thicknesses larger than 1nm<sup>14</sup>. As regards the APC, whether inconsistencies between the LSDA and experiment are due to some extrinsic phenomenon (e.g. disorder), or a failure in the LSDA, has remained an open question. The LSDA underestimates bandgaps, which strongly affects the band structure at imaginary  $k$  governing evanescent decay. It also poorly describes the Schottky barrier height<sup>23</sup>. Thus in the LSDA, most of the key parameters responsible for TMR are somewhat suspect.

Here we investigate electronic structure of (001) Fe/MgO/Fe using the Quasiparticle Self-consistent *GW* (QS*GW*) approximation for the electronic structure, which does not rely on the LSDA. We find significant corrections to energy and  $k$ -space character of the minority spin channel interface states. We investigate how these electronic structure corrections alter I-V characteristics in the APC, and account for available experimental results<sup>12,18</sup>. QS*GW* uses self-consistency to minimize the many-body part of the hamiltonian, thus allowing accurate determination of quasiparticle (QP) levels with low-order diagrams. It has been tested for a wide variety of bulk material systems and has been shown to be a good predictor of materials properties for many classes of compounds composed of elements throughout the periodic table<sup>19-21</sup>. It vastly improves on the accuracy of any existing DFT method, as well as standard implementations of *GW*, namely  $G_0W_0$  (1-shot) perturbations

around the LSDA. Also it surmounts problems of self-consistency inherent in a true self-consistent  $GW$  scheme. Self-consistency is particularly important in ionic compounds such as  $\text{MgO}$ <sup>20</sup>. Moreover, it may be necessary for reliable description of the metal/insulator interface since screening at the interface can be particularly important. For example, screening has been shown to strongly affect the molecular levels of benzene near a graphite interface<sup>22</sup>, a correlation effect not captured by a Kohn-Sham theory. As we show here, QSGW applied to this highly heterogeneous system appears to have the same uniform accuracy found in homogeneous materials systems.

We develop a formula to obtain the transmission probability  $T$  that avoids direct calculation of the tunneling via Landauer-Buttiker theory.  $T$  is parameterized by the local density of states (DOS) inside the tunneling layer. As we will show, it does an excellent job at reproducing the full Landauer-Buttiker transmission for a given one-body hamiltonian; it thus makes possible predictions of transport within the QSGW approximation. Used in conjunction with QSGW,  $T$  calculated in APC is in excellent agreement with observed I-V characteristics. This demonstrates that the observed TMR is not an artifact of imperfections at the interface, but an *intrinsic property* of it. An important corollary is that many-body corrections to the LSDA for electronic structure can have profound effect on transport properties. In this particular case the dominant correction to the LSDA is a shift in the IRS, of the same magnitude as a typical bias voltage. But generally speaking we can expect QSGW to describe electronic structure in inhomogeneous systems with vastly better accuracy than commonly adopted approaches and thus investigate implication of these corrections for transport.

Owing to heavy computational costs, the Fe/MgO interface is modeled in QSGW with a periodic slab of 5 Fe and 5 MgO layers ordered on the (001) plane. All results reported here adopt a generalized linear muffin-tin orbitals (LMTO) method<sup>20,21</sup>, and use the relaxed nuclear coordinates of the Fe/MgO interface from Ref.<sup>24</sup>.

Minority DOS of the Fe/MgO superlattice, projected on the Fe interfacial atom, and onto the oxygen atom in the second layer from the interface, are depicted in Fig. 1 calculated in LSDA,  $G_0W_0$ , and QSGW. For all three methods LSDA,  $G_0W_0$ , and QSGW two narrow peaks are seen, separated by  $\sim 0.15$  eV. The iron and oxygen projected DOS have similar shapes, indicating that these peaks originate from the same interface resonance states. These states fall near midgap in MgO and decay exponentially, the decay being more pronounced in QSGW and  $G_0W_0$  due to larger MgO band gap as compared to that of LSDA.

The LSDA puts one peak just at  $E_F$ , in agreement with several prior LSDA calculations<sup>13–17</sup>. There is a corresponding IRS resonance in QSGW and  $G_0W_0$ , but it falls at  $E_F + 0.12$  eV and  $E_F + 0.15$  eV correspondingly. This difference with LSDA is important: it is compa-

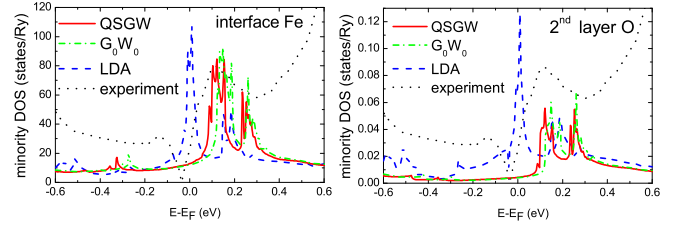


FIG. 1: (color online). Minority electron DOS projected to the surface Fe layer (left panel) and the oxygen atom in the second layer from the Fe/MgO interface (right panel). QSGW results are depicted by a (red) solid line,  $G_0W_0$  by (green) dash-dotted line, and LSDA by a (blue) dashed line. Note that the panels have different scales. Black dotted line depicts  $|d^2I/dV^2|$  measured in the antiparallel configuration<sup>12</sup> (arbitrary units).

table to typical bias voltages. Note that the iron and oxygen projected DOS obtained in  $G_0W_0$  is rather close to QSGW results. IRS peak in DOS of  $G_0W_0$  is just 0.03 eV higher in energy compared to QSGW, thus the energy shift from LSDA is mainly reproduced already at first GW iteration.

Through calculation of  $T$  we can establish a connection with I-V measurements (black dotted line in Fig. 1). The observed  $|d^2I/dV^2|$  has peaks at both  $+0.12$  V and  $-0.12$  V, with the former being more pronounced. The difference can be explained by the structural asymmetry<sup>12</sup>: the top interface is grown last and is rougher than the bottom one. In the following we show quantitatively that a combination of featureless DOS in the majority channel (not shown) and sharply peaked IRS states in the minority channel explains the observed peak in the differential conductance  $|d^2I/dV^2|$  at  $+0.12$  V. (Voltage is defined so that forward bias samples minority states of the bottom electrode with  $E > E_F$ ). We use the following expression for  $T$  at zero applied bias:

$$T_{\sigma\sigma'}^D(E) = \frac{\lambda}{N_{||}} \sum_{\mathbf{k}} \text{DOS}_{\mathbf{k}E}^{\sigma}(L) e^{-2\gamma_{\mathbf{k}E}d_{LR}} \text{DOS}_{\mathbf{k}E}^{\sigma'}(R) \quad (1)$$

$N_{||}$  is the number of  $\mathbf{k}$ -points in the 2D Brillouin zone normal to the interface,  $\sigma$  and  $\sigma'$  denote spin polarizations of the left and right electrodes,  $\text{DOS}_{\mathbf{k}E}^{\sigma}(L)$  is the DOS of electrons with spin  $\sigma$  projected onto nucleus  $L$ , chosen at will somewhere in the MgO close to the left Fe/MgO interface, and  $\text{DOS}_{\mathbf{k}E}^{\sigma'}(R)$  is the corresponding DOS of spin  $\sigma'$ , projected onto a nucleus  $R$  in MgO close to the right Fe/MgO interface.  $\gamma_{\mathbf{k}E}$  is the smallest (spin-independent) imaginary wave number for evanescent states inside the MgO barrier with given  $\mathbf{k}$  and energy  $E$ —a property of the complex band structure of bulk MgO.  $d_{LR}$  is the spacing between planes containing atoms  $L$  and  $R$ . Eqn. (1) neglects parallel channels with larger imaginary wave number, which is always satisfied if the barrier is thick enough. It becomes exact for one-dimensional case if the projected DOS is replaced by the

square of the wave function  $\psi$  propagating in corresponding electrode that is normalized to carry unit flux<sup>28,29</sup>. Since we replace the flux-normalized  $|\psi|^2$  with a local DOS, we include factor  $\lambda$  to correct for the (effectively unnormalized)  $\psi$ . Once local DOS and  $\gamma_{\mathbf{k}E}$  are given,  $T$  can be calculated for *arbitrary* MgO thickness. Though Eq. (1) bears a superficial resemblance to Jullière's formula, the latter takes into account only the spin polarization of electrodes, while Eq. (1) accounts for barrier-electrode coupling and evanescent decay as well. These contributions are the essential ones in the Fe/MgO system.

To evaluate the trustworthiness of Eq. (1), we compare it to a complete calculation of transmission within the Landauer-Buttiker formalism for a system with 4 MgO layers and semi-infinite Fe electrodes. For this purpose we use an implementation within the tight-binding LMTO method and Atomic Spheres Approximation (TB-LMTO-ASA)<sup>25,26</sup>. [As we show below the ASA is reasonably close to, but not identical with the full potential (FP) LSDA result; it matters little here since our purpose is to evaluate the reliability of Eq. (1)].

We first calculate transmission in APC,  $T_{AP}(E)$ , within the Landauer-Buttiker formalism, and compare to  $T_{AP}^D(E)$  from Eq. (1), staying within the TB-LMTO-ASA method. For  $T_{AP}^D(E)$  we employ DOS for a barrier containing 12 MgO layers (that ensures that local DOS is converged with thickness), and use for  $L$  and  $R$  respectively the O atom in the third layer from the left interface ( $L=O_3^L$ ) and the second layer from the right interface ( $R=O_2^R$ ). Thus the two DOS entering into Eq. (1) are  $\text{DOS}_{\mathbf{k}E}^{\text{maj}}(O_3^L)$  and  $\text{DOS}_{\mathbf{k}E}^{\text{min}}(O_2^R)$ .  $L=O_3^L$  and  $R=O_2^R$  because oxygen atoms have more valence electrons and are located closer to the interfacial Fe atoms; they thus better represent electrode-barrier coupling than do the Mg atoms. Also, for the 4-layer MgO barrier  $L=O_3^L$  and  $R=O_2^R$  is the same atom. Then  $d_{LR}=0$  and factor  $\gamma_{\mathbf{k}E}$  in Eq. (1) is not needed. As Fig. 2(a) shows,  $T_{AP}^D(E)$  is nearly identical with the Landauer-Buttiker  $T_{AP}(E)$  up to normalization  $\lambda$ . We also verified that DOS taken from O atoms in other choices of  $(L,R)$  pairs yield agreement between  $T_{AP}(E)$  and  $T_{AP}^D(E)$  comparable to that shown in Fig. 2(a). Thus, the trustworthiness of Eq. (1) is well established, and we can apply it with justification to the FP-LSDA and QSGW Hamiltonians.

The right panel of Fig. 2 shows  $T_{AP}^D(E)$ , assuming the same normalization  $\lambda$  ( $0.20 \text{ Ry}^2$ ) obtained by matching  $T_{AP}^D(E)$  to  $T_{AP}(E)$  in the ASA-LSDA approximation. The ASA calculation from the left panel is redrawn (blue solid line), and compared to a full-potential LSDA result (green dashed line). More precisely, the ASA approximation to  $\text{DOS}_{\mathbf{k}E}^{\text{min}}(O_2^R)$  is replaced by its analog calculated with a FP-LSDA method. Finally we obtain  $T_{AP}^D(\text{FP-QSGW})$  from  $\text{DOS}_{\mathbf{k}E}^{\text{min}}(O_2^R)$  calculated by QSGW in the repeated-slab geometry with 5 Fe and 5 MgO layers.

As Fig. 2 shows, the peak in  $T_{AP}^D$  falls near 0 V in both the ASA-LSDA and FP-LSDA cases, in agreement with earlier full-potential LSDA calculations<sup>15,17</sup>. The peak

of the QSGW-derived transmission is shifted to higher energy by approximately 0.12 eV relative to the  $T_{AP}^D(\text{FP-LSDA})$  result, putting it in close correspondence with the peak in  $|d^2I/dV^2|$  (measured in APC, shown as black dashed line on Fig. 2.  $|d^2I/dV^2|$  is shown rather than  $dI/dV$ , since the features are more easily seen<sup>12</sup>.) Note that  $T_{AP}^D(\text{QSGW}) < T_{AP}^D(\text{FP-LSDA})$ . This is because the LDA gap (4.7 eV) is much smaller than the experimental (7.8 eV) and QSGW (8.8 eV)<sup>20</sup> gaps; consequently  $\gamma_{\mathbf{k}E}$  is overestimated in the LDA. The transmission (not shown) obtained with  $G_0W_0$  minority DOS is very close to that obtained with QSGW minority DOS with shift of 0.03 eV to higher energy similar to that shown in Fig. 2.

Since finite-size effects of the leads can be important, we checked their sensitivity by calculating  $T_{AP}^D(\text{FP-LSDA})$  for slabs with 5, 7, and 9 Fe layers and 5, 7, and 9 MgO layers. We found that the peak position and general shape of  $T_{AP}^D$  depends weakly on the number of Fe and MgO layers. This is because minority IRS are mostly localized near the interface and their DOS quickly converges with number of Fe and MgO layers. On the other hand, finite size effects alter the majority DOS in the repeated-slab geometry. To eliminate finite-size effect in majority DOS we used the TB-LMTO-ASA majority  $\text{DOS}_{\mathbf{k}E}^{\text{maj}}(O_3^L)$  obtained for the semi-infinite electrode geometry and thick, 12-layer, MgO barrier for all three calculations. Since  $\text{DOS}_{\mathbf{k}E}^{\text{maj}}(O_3^L)$  is almost independent of energy on the scale we consider here ( $E_F \pm 0.4 \text{ eV}$ ), the shape and peak position of the  $T_{AP}^D(E)$  will not depend on whether ASA-LSDA, FP-LSDA, or FP-QSGW is used to evaluate  $\text{DOS}_{\mathbf{k}E}^{\text{maj}}(O_3^L)$  in the semi-infinite limit.

Significantly, there is only one peak in  $T$  in both the LSDA and QSGW approximations, despite the fact that two distinct peaks in the minority DOS appear (Fig. 1). To explain why only a single peak is seen, we analyze the QSGW DOS resolved by  $\mathbf{k}$  in the 2D Brillouin zone of the (001) plane. Fig. 3 shows the  $\mathbf{k}$  resolved DOS, at  $E_F + 0.12 \text{ eV}$  and  $E_F + 0.26 \text{ eV}$  (see two peaks in Fig. 1). As Fig. 3 shows, the  $\mathbf{k}$ -resolved DOS at  $E_F + 0.12 \text{ eV}$  is located mainly around the  $\Gamma$  point ( $\mathbf{k}=0$ ), while the DOS at the higher-energy peak ( $E_F + 0.26 \text{ eV}$ ) is concentrated near the zone boundary (this feature is common to QSGW and LDA). The conduction band of MgO is free-electron like, thus imaginary wave number depends on  $k$  approximately as  $\gamma(k) \approx \sqrt{k_0^2 + k^2}$ <sup>13</sup>. Nearly all the DOS weight for the high-energy peak occurs at large  $k$  where  $\gamma$  is large, so its contribution to  $T$  is effectively extinguished. This is in contrast to the low energy peak, where the surface DOS is concentrated at small  $k$ .

In conclusion, we developed a parametrization that reliably captures the essential elements of the tunneling process in magnetic tunnel junctions for any one-body hamiltonian. The tunneling probability derived from the QSGW approximation are in excellent agreement with observed differential conductance, in contrast to LSDA results. This confirms that the measured differential conductance peak is an intrinsic property of the ideal Fe/MgO (001) interface. This work also shows that cor-

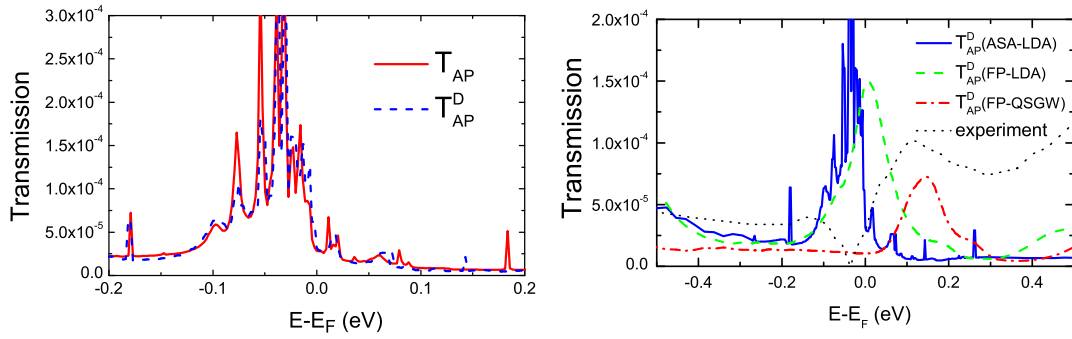


FIG. 2: (color online). Transmission function in the Fe/MgO system. Left:  $T_{AP}(E)$ , calculated in the APC by the TB-LMTO-ASA method for Fe/MgO/Fe MTJ with four MgO layers (red solid line) compared to the analytic formula  $T_{AP}^D(E)$ , Eq. (1) (blue dashed line), for a particular choice of sites in the MgO where local DOS is calculated. The latter was scaled by  $\lambda=0.20\text{Ry}^2$ . The quality of agreement is a measure of the quality of approximations used to obtain Eq. (1), as described in the text. We verified that the close correspondence between the analytic formula and the Landauer-Buttiker transmission seen in the left panel is insensitive to the choice of site chosen for the local DOS. Right:  $T_{AP}^D(E)$ , Eq. (1), calculated in the antiparallel configuration for several cases.  $T_{AP}^D$  shown in the left panel for the TB-LMTO-ASA method is redrawn as a (blue) solid line. The full-potential LSDA result is shown as a (green) dashed line.  $T_{AP}^D(E)$  from QSGW is shown as a (red) dash-dotted line. Experimental data (black dotted line) shows  $|d^2I/dV^2|$  measured in APC<sup>12</sup> (arbitrary units).

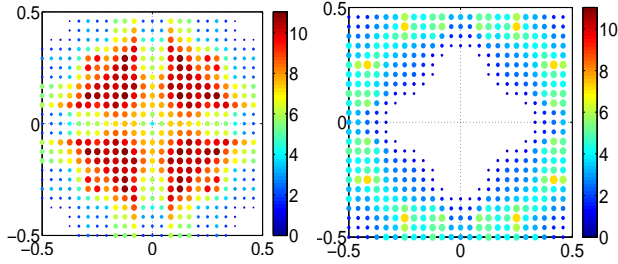


FIG. 3: (color online). The  $\mathbf{k}$ -resolved DOS of minority electrons projected to surface Fe layer calculated by QSGW for energies corresponding to the peaks in QSGW DOS, Fig. 1.

relations treated in the QSGW approximation are sufficient to realistically describe such metal insulator interfaces. Also, results obtained by  $G_0W_0$  and QSGW are very similar, indicating that in this system simple  $G_0W_0$  method is already sufficient to capture essential physical effects.

S.F. and O.N.M acknowledge the CNMS User support by Oak Ridge National Laboratory Division of Scientific User facilities and partial support by Seagate Technology. MvS was supported by ONR contract N00014-7-1-0479 and NSF QMHP-0802216.

\* Electronic address: sfaleev@nanotworks.com

† Electronic address: omryasov@mint.ua.edu

<sup>1</sup> International Technology Roadmap for Semiconductors (ITRS), 2009 Edition; <http://www.itrs.net/Links/2009ITRS/Home2009.htm>

<sup>2</sup> Hidenori Takagi and Harold Y. Hwang, Science **327**, 1600 (2010).

<sup>3</sup> J. Mannhart and D.G. Schlom, Science **327**, 1607 (2010).

<sup>4</sup> Hidenori Takagi and Harold Y. Hwang, Science **327**, 1601 (2010).

<sup>5</sup> Wolf S.A. et.al., Science **294**, 1488 (2001).

<sup>6</sup> Zutic I, Fabian J and Das Sarma S. Rev. Mod. Phys. **76**, 323 (2004).

<sup>7</sup> X.-G. Zhang and W.H. Butler, J. Phys.: Cond. Matt. **15**, R1603 (2003).

<sup>8</sup> E.Y. Tsymbal, O.N. Mryasov, and P.R. LeClair, J. Phys.: Condens. Matter **15**, R109 (2003).

<sup>9</sup> S. Yuasa, T. Nagahama, A. Fukushima, Y. Suzuki, and K. Ando, Nature Materials **3**, 868 (2004).

<sup>10</sup> S.S. P. Parkin, C. Kaiser, A. Panchula, P.M. Rice, and B. Hughes, Nature Materials **3**, 862 (2004).

<sup>11</sup> S. Yuasa and D.D. Djayaprawira, J. Phys. D: Appl. Phys. **40**, R337 (2007).

<sup>12</sup> P.-J. Zermatten, et al., Phys. Rev. B **78**, 033301 (2008)

<sup>13</sup> W. H. Butler, X.-G. Zhang, T. C. Schulthess, J. M. MacLaren, Phys. Rev. B **63**, 054416 (2001)

<sup>14</sup> K. D. Belashchenko, J. Velev, and E. Y. Tsymbal, Phys. Rev. B **72**, 140404(R) (2005)

<sup>15</sup> I. Rungger, O. Mryasov, and S. Sanvito, Phys. Rev. B, **79**, 094414 (2009)

<sup>16</sup> C. Tiisan et al., Phys. Rev. Lett. **93**, 106602 (2004).

<sup>17</sup> X. Feng, O. Bengone, M. Alouani, S. Lebegue, I. Rungger, and S. Sanvito, Phys. Rev. B **79**, 174414 (2009).

<sup>18</sup> G.X. Du, et al., Phys. Rev. B **81**, 064438 (2010)

<sup>19</sup> S. V. Faleev, M. van Schilfgaarde, and T. Kotani, Phys. Rev. Lett. **93**, 126406 (2004)

<sup>20</sup> M. van Schilfgaarde, T. Kotani, and S. V. Faleev, Phys. Rev. Lett. **96**, 226402 (2006)

<sup>21</sup> T. Kotani, M. van Schilfgaarde, and S. V. Faleev, Phys. Rev. B **76**, 165106 (2007)

<sup>22</sup> J.B. Neaton, M.S. Hybertsen, and S.G.Louie, Phys. Rev. Lett. **97**, 216405 (2006)

- <sup>23</sup> G. P. Das et al, Phys. Rev. Lett. **63**, 1168 (1989)
- <sup>24</sup> D. Worthmann, G. Bihlmayer, and S. Blugel, J. Phys.: Cond. Matt. **16**, S5819 (2004).
- <sup>25</sup> I. Turek, V. Drchal, J. Kudrnosky, M. Sob, P. Weinberger, *Electronic structure of disordered alloys, surfaces and interfaces*, (Kluwer, Boston, 1997)
- <sup>26</sup> M. van Schilfgaarde, W. R. L. Lambrecht, in *Tight-binding approach to computational materials science*, edited by L. Colombo, A. Gonis, and P. Turchi, MRS Symposia Proceedings No. 491 (Pittsburgh, 1998).
- <sup>27</sup> M. Jullière, Phys. Lett. A **54**, 225 (1975).
- <sup>28</sup> L.D. Landau and L.M. Lifshitz, *Quantum Mechanics*, Pergamon Press, Oxford, U.K.; New York, 1980.
- <sup>29</sup> K.D. Belashchenko et al., Phys. Rev. B **69**, 174408 (2004)